Coseismic deformations detectable by satellite gravity missions: A case study of Alaska (1964, 2002) and Hokkaido (2003) earthquakes in the spectral domain

Wenke Sun and Shuhei Okubo

Earthquake Research Institute, University of Tokyo, Tokyo, Japan

Received 24 April 2003; revised 4 February 2004; accepted 13 February 2004; published 10 April 2004.

[1] Coseismic deformations observed on the Earth surface or modeled by conventional dislocation theory cannot be compared directly with those observed by gravity satellite missions because of the spatial resolution limit of the missions and the signal attenuation of the gravity field. Coseismic deformations in the spectrum domain should be considered instead. For this purpose the conventional dislocation theory [e.g., *Sun and Okubo*, 1993] for a spherical Earth model can be used because it is expressed in the form of a spherical harmonic. In this study, analytical expressions of degree variances of the coseismic geoid and gravity changes for shear and tensile sources are derived and calculated for three real earthquakes. Those results are compared with expected errors of the Gravity Recovery and Climate Experiment (GRACE) to elucidate whether or not coseismic geoid and gravity changes are detectable by gravity satellite missions. Behaviors of the degree variances for four independent seismic sources are investigated. Results indicate that both the gravity and geoid changes are near two orders of magnitude larger than the precession of the gravity missions in low harmonic degrees. On the basis of these results, we derived the minimum magnitudes of earthquakes detectable by GRACE. We concluded that coseismic deformations for an earthquake with a seismic magnitude above $m = 7.5$ are expected to be detected by GRACE. *INDEX TERMS:* 1242 Geodesy and Gravity: Seismic deformations (7205); 1243 Geodesy and Gravity: Space geodetic surveys; 1214 Geodesy and Gravity: Geopotential theory and determination; 1299 Geodesy and Gravity: General or miscellaneous; 7260 Seismology: Theory and modeling; *KEYWORDS:* coseismic deformation, geoid, gravity, gravity mission, dislocation, earthquake

Citation: Sun, W., and S. Okubo (2004), Coseismic deformations detectable by satellite gravity missions: A case study of Alaska (1964, 2002) and Hokkaido (2003) earthquakes in the spectral domain, *J. Geophys. Res.*, *109*, B04405, doi:10.1029/2003JB002554.

1. Introduction

[2] Several dedicated satellite missions will continue to be available for gravity field determination from space. The Gravity Recovery and Climate Experiment (GRACE) [*National Research Council* (*NRC*), 1997] and the Gravity Field and Steady state Ocean Circulation Explorer (GOCE) [*European Space Agency* (*ESA*), 1999] are just two of them. They offer fundamental advantages over previous satellite missions: low-orbit altitude; uninterrupted tracking in three spatial dimensions; and measurement or compensation of nongravitational forces' effects. Use of GRACE allows measurement of temporal gravity variations caused by various geophysical processes. The primary objective of GRACE is to provide an unprecedented accurate, global, and high-resolution estimate of constant and time-variable components of the Earth's gravity field every 30 days over a 5 year period [*Wahr et al.*, 1998]. The main scientific objective of GOCE is to provide both high accuracy and a high spatial resolution gravity field and geoid model in a static sense. Some simulations [*ESA*, 1999] indicate that GOCE will dramatically improve the gravity model. The geoid accuracy will reach 1 cm for a half-wavelength of 100 km; the accuracy of gravity will be about 1 mgal [*ESA*, 1999]. The two missions are complementary. It is anticipated that the gravity missions will yield extremely wide geophysical applications in geosciences.

[3] Temporal gravity variations of global nature result from atmospheric mass redistribution, ocean circulation, polar ice melting or aggregation, the viscoelastic response of the Earth's lithosphere to past and present loads, etc. [*Chao et al.*, 2000; *Chao*, 2003]. In addition to these processes, earthquakes can produce significant global gravity perturbations that are detectable through analysis of gravity missions. A case study of the 1964 Alaska earthquake [*Sun and Okubo*, 1998] indicated that a gravity change was detectable on the Earth's surface by a superconducting gravimeter, even at epicentral distance of 5000 km. It also indicated that a geoid height change caused by the earthquake could reach 1.5 cm. However, it is questionable whether such gravity and geoid height changes can be detected by modern space techniques like altimetry and gravity missions. This question cannot be answered simply by results of surface gravity changes be-

0148-0227/04/2003JB002554$09.00

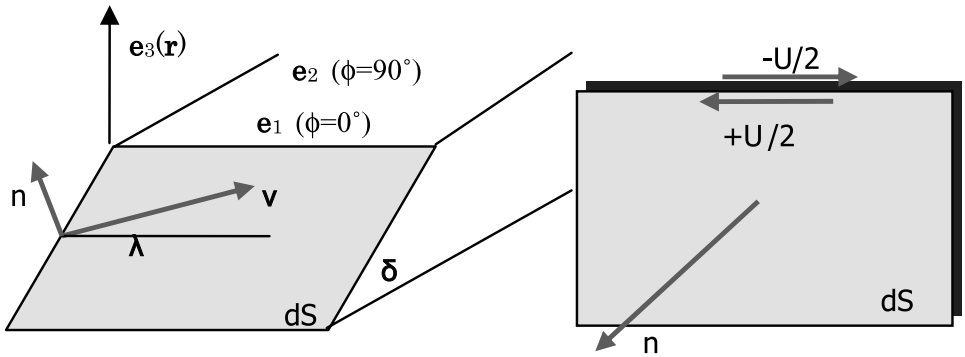

Figure 1. Dislocation slip vector **ν**, normal **n**, slip angle λ, and dip angle δ in the coordinate system ($\mathbf{e}_1$, $\mathbf{e}_2$, $\mathbf{e}_3$).

cause of their limited spatial resolution. On the other hand, coseismic gravity and geoid changes differ from other high-frequency variations such as Earth tides, which are expected to be large and coherent in nature. *Gross and Chao* [2001] investigated this problem using normal mode technique based on *Chao and Gross* [1987]. Comparing the degree amplitude spectra of some earthquakes with expected GRACE sensitivity, they concluded that coseismic effects of great earthquakes such as the 1960 Chilean or 1964 Alaska events can cause global gravitational field changes that are sufficiently large as to be detectable by GRACE. Mass redistribution in the Earth caused by an earthquake changes not only the gravity field, but also global rotation or polar motion. A related study can be found in *Chao et al.* [1996].

[4] In this study, we derive theoretical formulations of coseismic geoid and gravity changes and their degree variances, expressed by dislocation Love numbers. These expressions are achieved using dislocation theory, e.g., by *Sun and Okubo* [1993], for a spherical Earth as it is expressed in the form of spherical harmonics. We investigate coseismic geoid and gravity changes by observing the distribution of their degree variances in comparison to the expected sensitivity of satellite gravity missions. Results for coseismic deformations for large earthquakes are discussed with respect to their detectability. Note that this study offers an identical conclusion to that of *Gross and Chao* [2001] using the normal mode scheme.

2. Dislocation Theory and Dislocation Love Numbers

[5] Assume that an inclined point dislocation located on the polar axis in a compressible and self-gravitating spherical Earth. Furthermore, assume the fault line is in the direction of $\varphi = 0$ (Greenwich meridian). According to the quasi-static dislocation theory, coseismic geoid and gravity changes at an observation point (a, θ, φ) (see Figure 1) can be expressed as [*Sun and Okubo*, 1993]

$$\zeta^{ij}(a,\theta,\varphi) = \sum_{n,m} k^{ij}_{nm} Y^m_n(\theta,\varphi)\cdot \nu_i n_j \frac{UdS}{a^2} \tag{1}$$

$$\delta g^{ij}(a,\theta,\varphi) = \sum_{n,m} \left[(n+1)k^{ij}_{nm} - 2h^{ij}_{nm}\right]\cdot Y^m_n(\theta,\varphi)\nu_i n_j \frac{g_0 UdS}{a^3}, \tag{2}$$

where h^{ij}_{nm} (concerning the vertical displacement) and k^{ij}_{nm} (related to the gravitational potential change) are the dislocation Love numbers defined by *Sun and Okubo* [1993], functions of the spherical harmonic degree, order, source depth, and source type. Components of the slip vector and its normal on the infinitesimal fault area dS are ν_i and n_j, with total dislocation U. Gravity on the Earth surface is g_0; a is the radius of the Earth and Y^m_n (θ, φ) is the spherical harmonic function of degree n and order m. The two so-called dislocation factors, UdS/a^2 and g_0UdS/a^3, define the earthquake magnitude and give the unit of geoid and gravity changes.

[6] Notice that the gravity change in equation (2) involves the dislocation Love number h^{ij}_{nm}, which is related to vertical displacement. It can be removed form the formulation because satellites cannot detect this part of deformation. On the other hand, the current dislocation theory as given in equation (2) is derived based on the inner potential change which gives the factor (n + 1) for gravity change. The corresponding external potential should be used because we are interested in the gravity anomaly change (we still call it gravity change for convenience) outside the Earth. Thereby, equation (2) ultimately becomes

$$\delta g^{ij}(a,\theta,\varphi) = \sum_{n,m} (n-1)k^{ij}_{nm}\cdot Y^m_n(\theta,\varphi)\mathrm{n}_i n_j \frac{g_0 UdS}{a^3}. \tag{3}$$

A combination of the three slip and three normal components means that there are nine total solutions for all possible sources. However, only four independent solutions exist if the Earth model is spherically symmetric and isotropic. A deformation caused by an arbitrary source can be obtained by a proper combination of the four types of independent sources. In this study, we choose the following four independent solutions: ij = 12, 32, 22, and 33. They represent strike slip, dip slip, horizontal tensile and vertical tensile, respectively. Note that components of ij = 22 include two parts: m = 0 and 2; in this study, we calculate and discuss only the deformations of m = 0: the computation of m = 2 can be derived easily from the component of ij = 12. Details can be found in *Sun and Okubo* [1993] or *Sun et al.* [1996].

[7] Dislocation Love numbers k^{ij}_{nm} can be obtained numerically for a spherically symmetric Earth model [*Sun and Okubo*, 1993] such as the 1066A [*Gilbert and Dziewonski*, 1975] or the preliminary reference Earth model (PREM) [*Dziewonski and Anderson*, 1981]. Subsequently, gravity

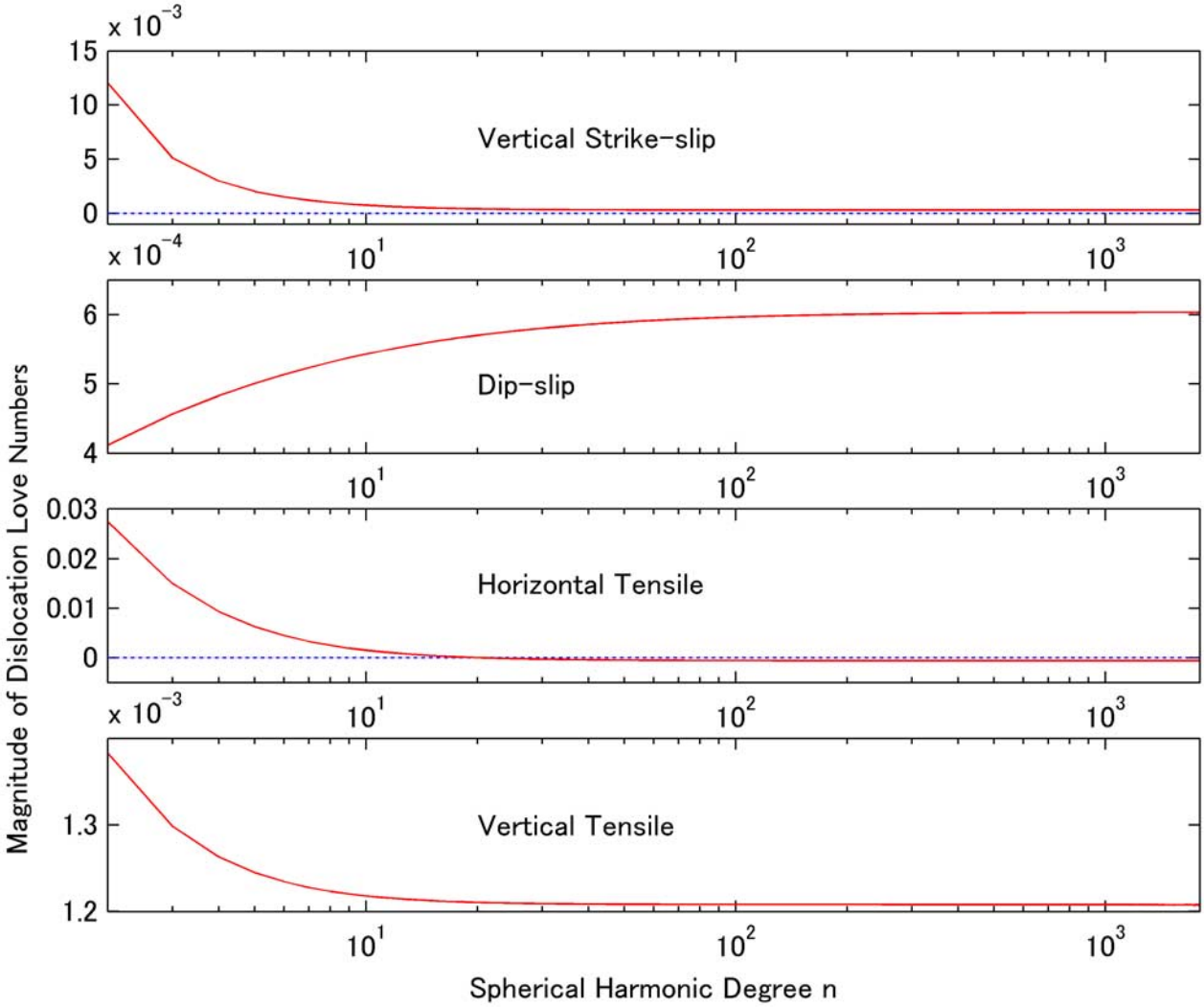

Figure 2. Normalized dislocation Love numbers k_{nm}^{ij} of four types of seismic sources at a depth of 32 km.

and geoid changes can be calculated by the above summations in equations (1) and (3). Figure 2 gives numerical results of the dislocation Love numbers k_{nm}^{ij} of the four types of seismic sources at a depth of 32 km with the 1066A model as a function of the spherical harmonic degree n up to 2000. The dislocation Love numbers vary rather smoothly as n increases. Once a dislocation source or earthquake parameter is provided, coseismic deformations can be calculated easily using these Love numbers.

3. Coseismic Geoid and Gravity Changes and Their Degree Amplitude Spectra

[8] A dislocation vector $\boldsymbol{\nu}$ and its normal $\mathbf{n}$ can be expressed in terms of dip angle δ and slip angle λ of the fault (Figure 1) as

$$\mathbf{n} = \mathbf{e}_3 \cos\delta - \mathbf{e}_2 \sin\delta \tag{4}$$

$$\boldsymbol{\nu} = \mathbf{e}_3 \sin\delta \sin\lambda + \mathbf{e}_1 \cos\lambda + \mathbf{e}_2 \cos\delta \sin\lambda. \tag{5}$$

We face a shear dislocation problem if the dislocation vector $\boldsymbol{\nu}$ runs parallel to the fault plan. Similarly, for a tensile opening, the dislocation vector $\boldsymbol{\nu}$ and its normal $\mathbf{n}$ become equal:

$$\boldsymbol{\nu} = \mathbf{n} = \mathbf{e}_3 \cos\delta - \mathbf{e}_2 \sin\delta. \tag{6}$$

Then for an arbitrary shear fault on the polar axis, according to equations (1) and (3) the coseismic geoid and gravity changes can be written as the following:

$$\begin{aligned}\zeta^{\text{Shear}}(a,\theta,\varphi) &= \sum_{i=1}^{3}\sum_{j=1}^{3}\zeta^{ij}(a,\theta,\varphi) \\ &= \sum_{n=2}^{\infty}\left\{\cos\lambda\left[-k_{n2}^{12}\sin\delta Y_n^2(\theta,\varphi) + k_{n1}^{13}\cos\delta Y_n^1(\theta,\varphi)\right]\right. \\ &\quad + \sin\lambda\left[\frac{1}{2}\left(k_{n0}^{33} - k_{n0}^{22}\right)\sin 2\delta Y_n^0(\theta,\varphi)\right. \\ &\quad \left.\left. + k_{n1}^{32}\cos 2\delta Y_n^1(\theta,\varphi)\right]\right\}\cdot\frac{UdS}{a^2}\end{aligned} \tag{7}$$

$$\delta g^{\text{Shear}}(a,\theta,\varphi) = \sum_{i=1}^{3}\sum_{j=1}^{3}\delta g^{ij}(a,\theta,\varphi)$$
$$= \sum_{n=2}^{\infty}\Big\{\cos\lambda\big[-(n-1)k_{n2}^{12}\sin\delta Y_n^2(\theta,\varphi) + (n-1)k_{n1}^{13}\cos\delta Y_n^1(\theta,\varphi)\big] + \sin\lambda\Big[\frac{1}{2}(n-1)\big(k_{n0}^{33}-k_{n0}^{22}\big)\sin 2\delta Y_n^0(\theta,\varphi) + (n-1)k_{n1}^{32}\cos 2\delta Y_n^1(\theta,\varphi)\Big]\Big\}\cdot\frac{g_0 UdS}{a^3}. \quad (8)$$

[9] Similarly, for a tensile source, the coseismic geoid and gravity changes become the following:

$$\zeta^{\text{Tensile}}(a,\theta,\varphi) = \sum_{i=1}^{3}\sum_{j=1}^{3}\zeta^{ij}(a,\theta,\varphi)$$
$$= \sum_{n=2}^{\infty}\Big[\big(k_{n0}^{33}\cos^2\delta + k_{n0}^{22}\sin^2\delta\big)Y_n^0(\theta,\varphi) - k_{n1}^{32}\sin 2\delta Y_n^1(\theta,\varphi)\Big]\cdot\frac{UdS}{a^2} \quad (9)$$

$$\delta g^{Tensile}(a,\theta,\varphi) = \sum_{i=1}^{3}\sum_{j=1}^{3}\delta g^{ij}(a,\theta,\varphi)$$
$$= \sum_{n=2}^{\infty}\Big[\big(k_{n0}^{33}\cos^2\delta + k_{n0}^{22}\sin^2\delta\big)(n-1)Y_n^0(\theta,\varphi) - k_{n1}^{32}\sin 2\delta(n-1)Y_n^1(\theta,\varphi)\Big]\cdot\frac{g_0 UdS}{a^3}. \quad (10)$$

We study coseismic deformations for each individual harmonic degree because the satellite gravity missions provide geoid and gravity measurements in the form of spherical harmonic coefficients, as pointed out by *Chao and Gross* [1987]. Consequently, it is straightforward to investigate whether coseismic deformations are detectable by the satellite gravity missions, e.g., GRACE. For this purpose, amplitude spectra of the above coseismic geoid and gravity changes in equations (7)–(10) will be computed for degrees $n = 2 - 100$. From equations (7)–(10) it can be seen that the terms of degrees $n = 0$ and $n = 1$ vanish because the total mass of the Earth is constant and the origin of the reference frame is located at the center of mass of the Earth model.

[10] On the other hand, it is known that, for a potential anomaly presented by a spherical harmonic series [*Heiskanen and Moritz*, 1967],

$$V(r,\theta,\varphi) = \frac{GM}{a}\sum_{n=0}^{\infty}\Big(\frac{a}{r}\Big)^{n+1}\sum_{m=-n}^{n}K_{nm}Y_n^m(\theta,\varphi)$$
$$= \frac{GM}{a}\sum_{n=0}^{\infty}\Big(\frac{a}{r}\Big)^{n+1}\sum_{m=-n}^{n}(C_{nm}\cos m\varphi + S_{nm}\sin m\varphi)P_n^m(\sin\theta). \quad (11)$$

The degree variance c_n^2 (i.e., the power spectral density) of the gravitational potential anomaly, which gives the contribution of the degree n terms to the total variance, is defined as [*ESA*, 1999]

$$c_n^2 = \sum_{m=0}^{n}\big(C_{nm}^2 + S_{nm}^2\big) = \sum_{m=-n}^{n}|K_{nm}|^2. \quad (12)$$

That is also known as the root-mean-square value per degree. Comparing equations (7)–(10) to equation (11) indicates that the coefficients (the dislocation love numbers and the geographical parameters of the fault) of $Y_n^m(\theta,\varphi)$ in equations (7)–(10) are nothing but the Stokes coefficients. The angular order m vanishes except $m = 0$, 1 and 2 because the source is chosen at the polar axis and also because of the symmetric property of the source functions. Therefore the computation of the degree variance is slightly easier than the full spectrum-distributed coefficients. The degree variances for shear and tensile sources can be written straightforwardly as the following equations:

$$\big(c_n^{\text{Shear}}\big)_\zeta^2 = \Big[\big(k_{n2}^{12}\sin\delta\cos\lambda\big)^2 + \big(k_{n1}^{13}\cos\delta\cos\lambda\big)^2 + \Big(\frac{1}{2}k_{n0}^{22}\sin 2\delta\sin\lambda\Big)^2 + \Big(\frac{1}{2}k_{n0}^{33}\sin 2\delta\sin\lambda\Big)^2 + \big(k_{n1}^{32}\cos 2\delta\sin\lambda\big)^2\Big]\cdot\Big(\frac{UdS}{a^2}\Big)^2, \quad (13)$$

$$\big(c_n^{\text{Shear}}\big)_{\delta g}^2 = \Big[\big(k_{n2}^{12}\sin\delta\cos\lambda\big)^2 + \big(k_{n1}^{13}\cos\delta\cos\lambda\big)^2 + \Big(\frac{1}{2}k_{n0}^{22}\sin 2\delta\sin\lambda\Big)^2 + \Big(\frac{1}{2}k_{n0}^{33}\sin 2\delta\sin\lambda\Big)^2 + \big(k_{n1}^{32}\cos 2\delta\sin\lambda\big)^2\Big]\cdot(n-1)^2\Big(\frac{g_0 UdS}{a^3}\Big)^2, \quad (14)$$

$$\big(c_n^{\text{Tensile}}\big)_\zeta^2 = \Big[\big(k_{n0}^{33}\cos^2\delta\big)^2 + \big(k_{n0}^{22}\sin^2\delta\big)^2 + \big(k_{n1}^{32}\sin 2\delta\big)^2\Big]\cdot\Big(\frac{UdS}{a^2}\Big)^2, \quad (15)$$

$$\big(c_n^{\text{Tensile}}\big)_{\delta g}^2 = \Big[\big(k_{n0}^{33}\cos^2\delta\big)^2 + \big(k_{n0}^{22}\sin^2\delta\big)^2 + \big(k_{n1}^{32}\sin 2\delta\big)^2\Big]\cdot(n-1)^2\Big(\frac{g_0 UdS}{a^3}\Big)^2. \quad (16)$$

It is seen that the degree variances involve not only the dislocation Love numbers, but also the geometrical position of the fault described by the dip angle ζ and slip angle λ, and the dislocation factors. It is also found that the degree variances for a shear fault movement include both the shear and tensile components; whereas the degree variances for a tensile fault also include the two components, but are unconnected with the dip angle.

[11] In practical calculation, parameters such as source type ij and harmonic order m are determined according to the selected source types. For example, for a vertical strike-slip fault, $ij = 12$, $m = 2$, $\delta = 90°$ and $\lambda = 90°$. Then for the

four independent sources, the degree variances can be simplified as the following formulas:

$$\left(c_n^{12}\right)_{\varsigma} = \left|k_{n2}^{12}\right| \frac{UdS}{a^2}, \tag{17}$$

$$\left(c_n^{32}\right)_{\varsigma} = \left|k_{n1}^{32}\right| \frac{UdS}{a^2}, \tag{18}$$

$$\left(c_n^{22}\right)_{\varsigma} = \left|k_{n0}^{22}\right| \frac{UdS}{a^2}, \tag{19}$$

$$\left(c_n^{33}\right)_{\varsigma} = \left|k_{n0}^{33}\right| \frac{UdS}{a^2}, \tag{20}$$

$$\left(c_n^{12}\right)_{\delta g} = (n-1)\left|k_{n2}^{12}\right| \frac{g_0 UdS}{a^3}, \tag{21}$$

$$\left(c_n^{32}\right)_{\delta g} = (n-1)\left|k_{n1}^{32}\right| \frac{g_0 UdS}{a^3}, \tag{22}$$

$$\left(c_n^{22}\right)_{\delta g} = (n-1)\left|k_{n0}^{22}\right| \frac{g_0 UdS}{a^3}, \tag{23}$$

$$\left(c_n^{33}\right)_{\delta g} = (n-1)\left|k_{n0}^{33}\right| \frac{g_0 UdS}{a^3}. \tag{24}$$

Equations (17)–(24) show that the degree variances are proportional to the absolute values of the dislocation Love numbers because they are functions of one of the three angular orders 0, 1, or 2. For each harmonic degree n, the only variable is the dislocation Love number, so that the root-square of the dislocation number is its absolute value. Therefore the dislocation Love numbers themselves give their degree variances, multiplied by the dislocation factors that are determined by a selected earthquake. These degree variances can be obtained easily from the above dislocation Love numbers in Figure 2.

4. Degree Amplitude of the Four Independent Sources

[12] We first consider a great fault equivalent to that of the Alaska earthquake (1964, m_w = 9.2) with parameters of [*Savage and Hastie*, 1966] 600 km length, 200 km width, 20 km depth, and 10 m dislocation. The degree variances are computed for the above four independent types of sources. Thereby, we can observe behaviors of respective sources. The dislocation factors in equations (7)–(10) yield UdS/a^2 = 29.56 mm for geoid change and g_0UdS/a^3 = 4.556 μgal for gravity change. Consequently, the degree variances of the four source types can be written easily from equations (17)–(24) as the following relationships:

$$\left(c_n^{12}\right)_{\varsigma} = 29.56\left|k_{n2}^{12}\right|(\text{mm}),$$

$$\left(c_n^{32}\right)_{\varsigma} = 29.56\left|k_{n1}^{32}\right|(\text{mm}),$$

$$\left(c_n^{22}\right)_{\varsigma} = 29.56\left|k_{n0}^{22}\right|(\text{mm}),$$

$$\left(c_n^{33}\right)_{\varsigma} = 29.56\left|k_{n0}^{33}\right|(\text{mm}),$$

$$\left(c_n^{12}\right)_{\delta g} = 4.556(n-1)\left|k_{n2}^{12}\right|(\mu\text{gal}),$$

$$\left(c_n^{32}\right)_{\delta g} = 4.556(n-1)\left|k_{n1}^{32}\right|(\mu\text{gal}),$$

$$\left(c_n^{22}\right)_{\delta g} = 4.556(n-1)\left|k_{n0}^{22}\right|(\mu\text{gal}),$$

$$\left(c_n^{33}\right)_{\delta g} = 4.556(n-1)\left|k_{n0}^{33}\right|(\mu\text{gal}).$$

Correspondingly, degree variances of the geoid and gravity components for the four sources are calculated and plotted in Figures 3 and 4, respectively. Those figures also show the expected instrument errors of the GRACE measurements [*Gross and Chao*, 2001] of these quantities.

[13] The relative contribution to each component of the geoid and gravity changes can be seen clearly from Figures 3 and 4 by observing the magnitude distribution of these degree variances. An important property shown in Figures 3 and 4 is that the two tensile sources have stronger power than the two shear sources. This property means that coseismic deformations of the tensile sources are expected to be larger than those of the shear sources. It implies that even for the same geographical fault size (or moment) of an earthquake, their contributions to geoid and gravity changes may be different. Comparing the degree variances with the GRACE error indicates that GRACE can detect the coseismic geoid and gravity changes for the two tensile sources because they are almost two orders larger in magnitude until the first 70 degrees. The geoid and gravity changes for the two shear sources are all equal to or less than the GRACE error; also, they are difficult to detect. Figures 3 and 4 also show that the degree strength has a different contribution at different harmonic degree n. The degree variance of vertical strike-slip source decreases rapidly as degree n increases.

[14] Table 1 shows that we may easily derive the minimum magnitudes of earthquakes which are expected to be detected by the gravity missions according to the above results and discussions. It indicates that if an earthquake is as large as the magnitude of m = 9.0 (for source types 12 and 32) or m = 7.5 (for source types 22 and 33), the corresponding coseismic deformations are expected to be detected by GRACE. Note that the coseismic geoid and gravity changes are expected to be easily detected by the future GRACE follow-on. If it offers about two orders better accuracy than GRACE [*Watkins et al.*, 2000; *NRC*, 1997],

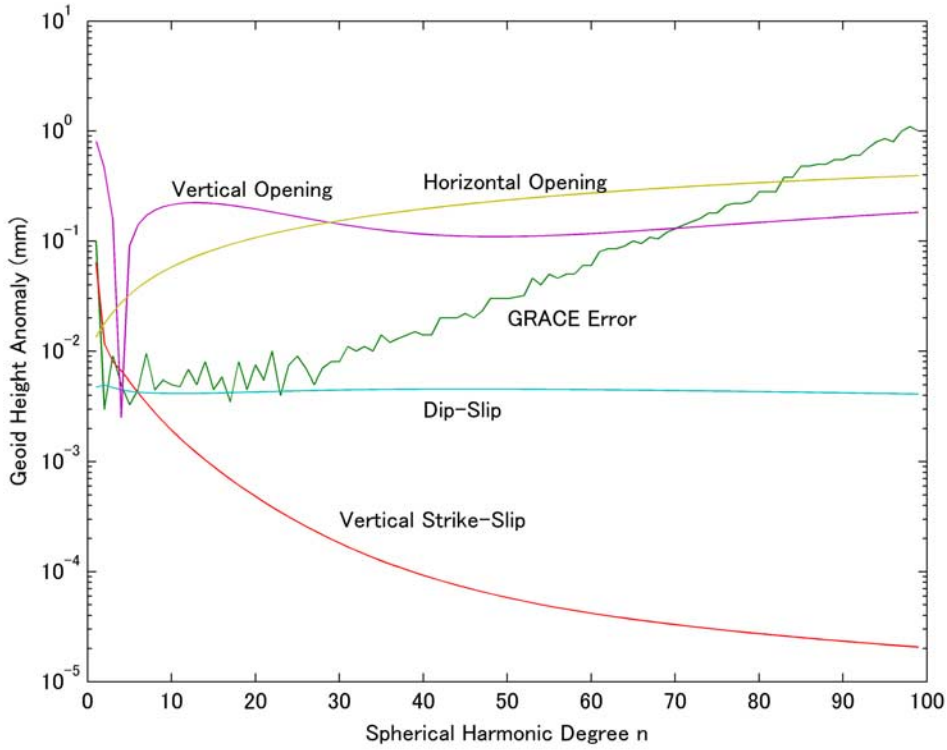

Figure 3. Degree amplitude spectra for the coseismic geoid height changes caused by four types of sources at 20 km depth in the 1066A Earth model: vertical strike slip, dip slip, horizontal opening (tensile), and vertical opening. The parameters of the Alaska earthquake (1964, m_w = 9.2) are 600 km length, 200 km width, 20 km depth, and 10 m dislocation. The dislocation factor of geoid change is UdS/a^2 = 29.56 mm. Expected instrument errors of the Gravity Recovery and Climate Experiment (GRACE) are also plotted.

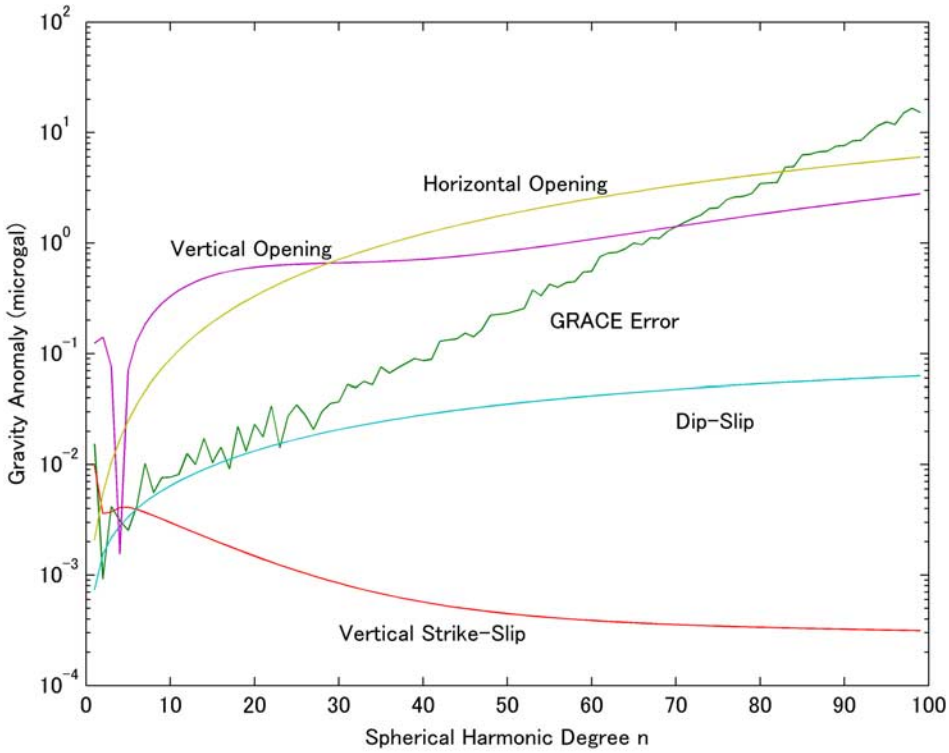

Figure 4. Same as Figure 3, but for gravity.

Table 1. Minimum Magnitude of Earthquakes Expected to be Detected by the Gravity Recovery and Climate Experiment (GRACE)

Source Type *ij*	Minimum Seismic Magnitude (*m*)
12	9.0
32	9.0
22	7.5
33	7.5

the minimum magnitude of earthquakes expected to be detected by GRACE follow-on is $m = 7.5$ for source types 12 and 32 or $m = 6.0$ for source types 22 and 33.

5. Case Study: Alaska Earthquakes (1964, 2002) and the Hokkaido (2003) Earthquake

[15] In this section, as a case study, let us consider three actual earthquakes: the Alaska earthquakes occurred in 1964 ($m_w = 9.2$) and in 2002 ($m = 7.9$), and the Hokkaido (Japan) earthquake happened in 2003 ($m = 8.0$). Table 2 lists fault parameters of these three earthquakes. We can learn whether the coseismic geoid and gravity can be detected by observing their degree variances in comparison to the GRACE error. For this purpose, we derive formulas describing the degree variances of the three earthquakes.

5.1. Case 1: The 1964 Alaska Earthquake

[16] According to the parameters in Table 1, it is known that $\delta = 9°$ and $\lambda = 90°$, $UdS/a^2 = 29.56$ mm and $g_0UdS/a^3 = 4.556$ μgal. The degree variances of geoid and gravity changes can be written as equation (25) because it is a dip-slip source with a low dip angle. From equations (13) and (14),

$$\left(c_n^{\text{Shear}}\right)_\zeta^2 = \left[\left(\frac{1}{2}k_{n0}^{22}\sin 18°\right)^2 + \left(\frac{1}{2}k_{n0}^{33}\sin 18°\right)^2 + \left(k_{n1}^{32}\cos 18°\right)^2\right] \cdot (29.56\text{ mm})^2 \tag{25}$$

$$\left(c_n^{\text{Shear}}\right)_{\delta g}^2 = \left[\left(\frac{1}{2}k_{n0}^{22}\sin 18°\right)^2 + \left(\frac{1}{2}k_{n0}^{33}\sin 18°\right)^2 + \left(k_{n1}^{32}\cos 18°\right)^2\right] \cdot (n-1)^2(4.556\ \mu\text{gal})^2. \tag{26}$$

5.2. Case 2: The 2002 Alaska Earthquake

[17] According to parameters in Table 1, we have $\delta = 90°$ and $\lambda = 0°$, $UdS/a^2 = 0.6356$ mm and $g_0UdS/a^3 = 0.0980$ μgal. The degree variances of geoid and gravity changes can be simplified as equation (27) because it is a vertical strike-slip source. From equations (13) and (14),

$$\left(c_n^{\text{Shear}}\right)_\zeta^2 = \left(k_{n2}^{12}\right)^2 \cdot (0.6356\text{ mm})^2 \tag{27}$$

$$\left(c_n^{\text{Shear}}\right)_{\delta g}^2 = \left(k_{n2}^{12}\right)^2 (n-1)^2 (0.0980\ \mu\text{gal})^2. \tag{28}$$

5.3. Case 3: The 2003 Hokkaido Earthquake

[18] In this case, $UdS/a^2 = 0.4100$ mm and $g_0UdS/a^3 = 0.0630$ μgal from equations (13) and (14), $\delta = 20°$ and $\lambda = 90°$. Degree variances of geoid and gravity changes are

$$\left(c_n^{\text{Shear}}\right)_\zeta^2 = \left[\left(\frac{1}{2}k_{n0}^{22}\sin 40°\right)^2 + \left(\frac{1}{2}k_{n0}^{33}\sin 40°\right)^2 + \left(k_{n1}^{32}\cos 40°\right)^2\right] \cdot (0.4100\text{ mm})^2 \tag{29}$$

$$\left(c_n^{\text{Shear}}\right)_{\delta g}^2 = \left[\left(\frac{1}{2}k_{n0}^{22}\sin 40°\right)^2 + \left(\frac{1}{2}k_{n0}^{33}\sin 40°\right)^2 + \left(k_{n1}^{32}\cos 40°\right)^2\right] \cdot (n-1)^2(0.0630\ \mu\text{gal})^2. \tag{30}$$

Subsequently, the degree variances from equations (25) to (30) are calculated using the dislocation numbers given in Figure 1 and plotted in Figures 5 and 6for the geoid and gravity changes, respectively. The GRACE errors are also plotted in the figures for comparison.

[19] Figures 5 and 6 show that the 1964 Alaska earthquake causes the coseismic geoid and gravity changes in low degree part with near two orders in magnitude larger than the GRACE error. This fact indicates that the global geoid and gravity changes are sufficiently large to be detected by GRACE. The figures also show that the geoid and gravity changes caused by the 2002 Alaska earthquake and the 2003 Hokkaido earthquake are smaller than the GRACE error: apparently, they are too small to be detected by GRACE. Although the geoid and gravity effects at degree 3 show the same level with the GRACE error, considering other physical effects and the rather long measurement period (one month), they are less likely to be detected in actual practice. Note that results of the 1964 Alaska earthquake show the same property as that given by *Gross and Chao* [2001].

[20] Comparison of the degree variances of the 2002 Alaska and the 2003 Hokkaido earthquakes showed that geoid and gravity effects for the 2003 Hokkaido earthquakes are much larger than those of the 2002 Alaska earthquake at almost all the harmonic degrees, but that their fault sizes are almost identical. This fact further confirms that the geographical position, especially the dip angle,

Table 2. Parameters of Three Earthquakes

Location	Length, km	Width, km	Dislocation, m	Depth, km	Slip Angle, deg	Dip Angle, deg
Alaska (1964)	600	200	10	20	90	9
Alaska (2002)	200	30	4.3	15	0	90
Hokkaido (2003)	80	80	2.6	15	90	20

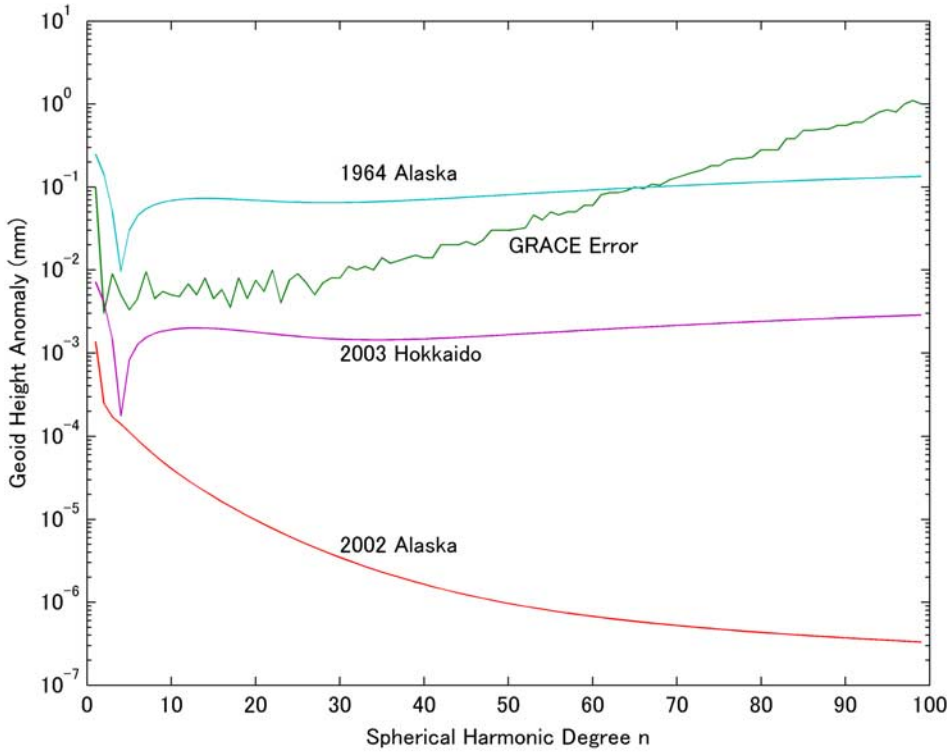

Figure 5. Degree amplitude spectra for the coseismic geoid height changes caused by three earthquakes: the 1964 Alaska (9.2), the 2002 Alaska (7.9), and the 2003 Hokkaido (8.0). Table 1 lists parameters of the three earthquakes. Expected instrument errors of GRACE are also plotted.

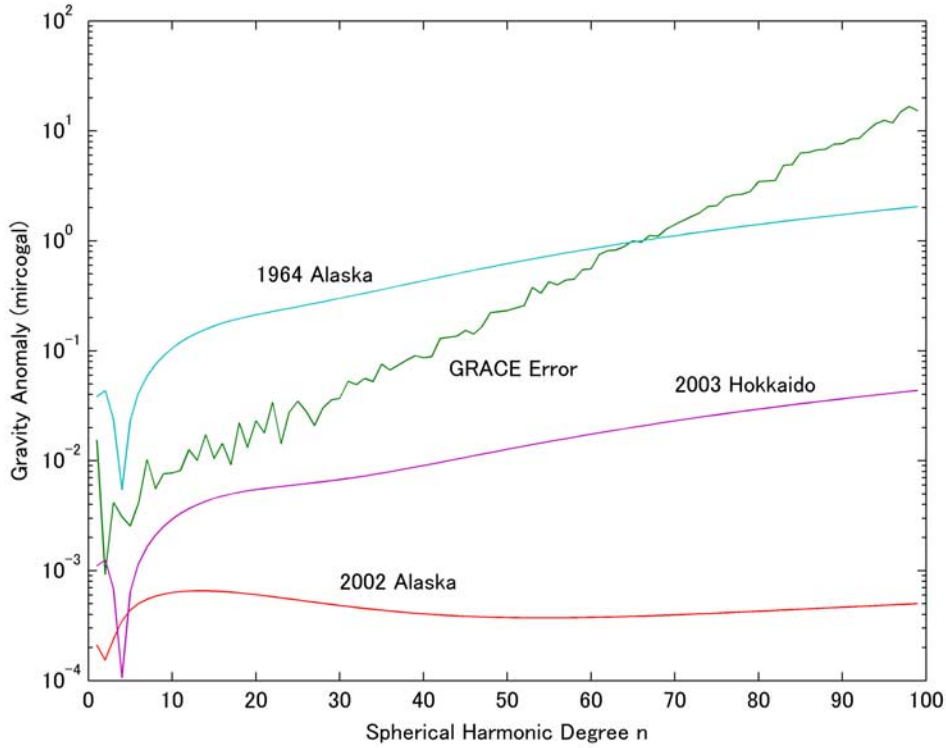

Figure 6. Same as Figure 5, but for gravity.

plays an important role in these geophysical effects. This importance is understandable: the dip slip source involves tensile components, which are shown to be much larger than the shear sources.

[21] Note that the above results represent coseismic deformations of a point source (dislocation). In practice, if the fault size is extremely large or compatible with the distance between the source and satellite, the geometrical shape of the fault should be considered. A point source is sufficient if the fault size is sufficiently small in comparison to the distance from satellite to the Earth surface. The source depth is another factor affecting the magnitude of deformations. Nevertheless, the effect of source depth is considered to be relatively small compared to the fault size because coseismic deformation, especially the geoid change, is relatively less sensitive to depth [*Sun and Okubo*, 1998]. Note that the finite size of the fault might be important for the GRACE follow-on mission. To reduce contamination from hydrology, oceanography, and other factors, we address extremely small regions because relatively small follow-on errors will permit us to examine such small regions. Those regions should be sufficiently small that the fault size plane extent for a large event could be important. An integration of a point source over the fault plane is required to compute accurate coseismic deformations by a limited fault size. However, this study is intended to observe the magnitude of coseismic deformations. For that reason, a rough approximation is acceptable.

[22] We emphasize that coseismic gravity changes are difficult to distinguish in practice because of complications of the gravity field. Ideally, to distinguish coseismic geoid and gravity changes, the gravity field should be observed just before and after the seismic event. In this case, all other long temporal effects on gravity change should be relative small and can therefore be neglected. In practice, however, GRACE provides us with a complete gravity observation in a one month time interval. During that one month, the Earth undergoes many geophysical changes that engender temporal gravity changes. In other words, the temporal gravity variations are expected to comprise many physical effects such as tidal changes, atmospheric changes, rain or snow fall, and so on. On the other hand, in some timescale, other temporal gravity variations are equal in size, or even larger than, the coseismic deformations. Therefore all of these gravity changes should be well modeled or observed before the coseismic gravity changes can be detected.

[23] The above results and discussions imply that coseismic geoid and gravity changes are almost impossible to detect by GRACE. However, for an earthquake with a magnitude greater than $m = 7.9$, such as $m > 8.0$, as shown in Table 1, coseismic geoid and gravity changes are anticipated to be detectable by GRACE. On a hopeful note, geoid and gravity changes caused by the equivalent of the 2002 Alaska earthquake may be detectable from space by projects like the GRACE follow-on mission because the forthcoming GRACE follow-on gravity mission is expected to have better accuracy, by more than two orders, than GRACE.

6. Summary

[24] Coseismic deformations observed on the Earth surface or modeled by conventional dislocation theory cannot be compared directly with those observed by satellite gravity missions because of the spatial resolution limit of the gravity satellites and the signal attenuation of the gravity field. Instead, coseismic deformations in the spectral domain should be considered so that the deformations can be investigated by individual spherical harmonic degrees. This method demands theoretical investigation of dislocation theory. For this purpose, the conventional dislocation theory for a spherical Earth model, e.g., the theory of *Sun and Okubo* [1993] can be used as it is expressed in the form of a spherical harmonic. Coseismic deformations can be estimated using the theory with a spherical harmonic form. Degree variances of the coseismic geoid and gravity changes for shear and tensile sources are derived analytically. Numerical investigation was carried out to observe whether coseismic geoid and gravity changes are detectable by satellite gravity missions. Numerical results of the degree variances were used for comparison with the expected sensitivity of the gravity missions. A seismic source equivalent to the fault size of the great Alaska earthquake (1964, $m_w = 9.2$) was adopted for practical calculation. Then, we undertook case studies of Alaska (1964, 2002) and Hokkaido earthquakes [2003]. The corresponding modeled coseismic deformations indicated that both gravity and geoid changes are near two orders larger than the GRACE precession. This study derived minimum earthquakes to be detected by GRACE mission. The results engender the conclusion that coseismic deformations for an earthquake with a seismic magnitude of $m = 7.5$ are expected to be detectable by GRACE. Of course, these conclusions depend upon and vary according to source depth and type. Finally, it is notable that this study addresses only part of the broader question of whether gravity satellite missions can detect coseismic geoid and gravity variations. The question remains whether the seismic signal will rise above other time-variable gravity signals from hydrology, oceanography, and so on. The observed gravity signal is an integrated one. For that reason, we must examine all possible physical sources and carefully model each of them to distinguish individual contributions and thereby correctly interpret time-variable gravity.

[25] **Acknowledgments.** The authors are grateful for comments by B. F. Chao, R. Gross, and an anonymous reviewer, all of which improved the manuscript greatly. This research was supported financially by JSPS research grants (C13640420) and "Basic design and feasibility studies for the future missions for monitoring Earth's environment."

References

Chao, B. F. (2003), Geodesy is not just for static measurements any more, *Eos Trans. AGU*, *84*, 145, 150.

Chao, B. F., and R. S. Gross (1987), Changes in the Earth's rotation and low-degree gravitational field induced by earthquakes, *Geophys. J. R. Astron. Soc.*, *91*, 569–596.

Chao, B. F., R. S. Gross, and Y. Han (1996), Seismic excitation of the polar motion, 1977–1993, *Pure Appl. Geophys.*, *146*, 407–419.

Chao, B. F., V. Dehant, R. S. Gross, R. D. Ray, D. A. Salstein, M. M. Watkins, and C. R. Wilson (2000), Space geodesy monitors mass transports in global geophysical fluids, *Eos Trans. AGU*, *81*, 247, 249–250.

Dziewonski, A. M., and D. L. Anderson (1981), Preliminary Reference Earth Model, *Phys. Earth Planet. Inter.*, *25*, 297–356.

European Space Agency (ESA) (1999), Gravity field and steady-state ocean circulation mission: Reports for mission selection: The four candidates Earth explorer core missions, *Rep. SP-1233 (1)*, Noordwijk, Netherlands.

Gilbert, F., and A. M. Dziewonski (1975), An application of normal mode theory to the retrieval of structural parameters and source mechanisms from seismic spectra, *Philos. Trans. R. Soc. London, Ser. A*, *278*, 187–269.

Gross, R. S., and B. F. Chao (2001), The gravitational signature of earthquakes, in *Gravity, Geoid and Geodynamics: GGG2000 IAG International Symposium, Banff, Alberta, Canada, July 31–August 4, 2000*, vol. 123, edited by M. G. Sideris, pp. 205–210, Springer-Verlag, New York.

Heiskanen, W. A., and H. Moritz (1967), *Physical Geodesy*, W. H. Freeman, New York.

National Research Council (NRC) (1997), *NAS, Satellite Gravity and the Geosphere*, edited by J. O. Dickey, Washington, D. C.

Savage, J. C., and L. M. Hastie (1966), Surface deformation associated with dip-slip faulting, *J. Geophys. Res.*, *71*, 4897–4904.

Sun, W., and S. Okubo (1993), Surface potential and gravity changes due to internal dislocations in a spherical Earth, I. Theory for a point dislocation, *Geophys. J. Int.*, *114*, 569–592.

Sun, W., and S. Okubo (1998), Surface potential and gravity changes due to internal dislocations in a spherical Earth, II. Application to a finite fault, *Geophys. J. Int.*, *132*, 79–88.

Sun, W., S. Okubo, and P. Vaníček (1996), Global displacements caused by dislocations in a realistic Earth model, *J. Geophys. Res.*, *101*, 8561–8577.

Wahr, J., M. Molenaar, and F. Bryan (1998), Time variability of the Earth's gravity field: Hydrological and oceanic effects and their possible detection using GRACE, *J. Geophys. Res.*, *103*, 30,205–30,230.

Watkins, M. M., W. M. Folkner, B. F. Chao, and B. D. Tapley (2000), The NASA EX-5 mission: A laser interferometer follow-on to GRACE, paper presented at the GGG2000 International Symposium, Int. Assoc. Geod., Banff, Alberta, Canada, 31 July–4 Aug.

S. Okubo and W. Sun, Earthquake Research Institute, University of Tokyo, Yayoi 1-1-1, Bunkyo-ku, Tokyo 113-0032, Japan. (okubo@eri.u-tokyo.ac.jp; sunw@eri.u-tokyo.ac.jp)